

# MIMO Channel Capacity and Configuration Selection for Switched Parasitic Antennas

Paramvir Kaur Pal and Robert Simon Sherratt

**Multiple-input multiple-output (MIMO) systems offer significant enhancements in terms of their data rate and channel capacity compared to traditional systems. However, correlation degrades the system performance and imposes practical limits on the number of antennas that can be incorporated into portable wireless devices. The use of switched parasitic antennas (SPAs) is a possible solution, especially where it is difficult to obtain sufficient signal decorrelation by conventional means. The covariance matrix represents the correlation present in the propagation channel, and has significant impact on the MIMO channel capacity. The results of this work demonstrate a significant improvement in the MIMO channel capacity by using SPA with the knowledge of the covariance matrix for all pattern configurations. By employing the “water-pouring algorithm” to modify the covariance matrix, the channel capacity is significantly improved compared to traditional systems, which spread transmit power uniformly across all the antennas. A condition number is also proposed as a selection metric to select the optimal pattern configuration for MIMO-SPAs.**

**Keywords:** Condition number, Eigenvalue spread, MIMO, Switched parasitic antennas.

## I. Introduction

Multiple-input multiple-output (MIMO) systems employ multiple transmit and receive antennas to improve the channel capacity and data rates using multiplexing, without increasing the transmit power or bandwidth [1], [2]. The performance enhancements obtained through MIMO techniques come at the expense of implementing multiple antennas, which occupy more space and have higher power requirements. It also increases the hardware complexity for multi-dimensional signal processing. Although MIMO systems are capable of providing the expected data rates theoretically, it is often not possible in practice owing to the spatial correlation between antennas [2]. Generating multiple spatial streams requires uncorrelated paths for each stream through the propagation medium, such that the individual streams arrive at the receiver with sufficiently distinct spatial signatures. A solution to all of these problems is to employ antennas with different radiation patterns by using switched parasitic antennas (SPAs) [3]–[5], which makes pattern diversity attractive in the design of small user terminals for MIMO communication systems. In portable communication devices, the use of SPAs reduces cost, power consumption, and hardware complexity.

The working principle of MIMO using SPA is based on electromagnetic coupling between all of the elements, and the beam-pattern is controlled by switching the loads of parasitic elements. In MIMO-SPA, few active elements are connected to the RF chains, and they are surrounded by some parasitic elements terminated with impedances loads. By modifying the controllable impedance loads, parasitic elements can be set in and out of resonance. These antennas are capable of dynamically changing their radiation properties by means of RF switches used to vary the current distribution on the antenna array structure.

---

Manuscript received June 6, 2017; revised Nov. 8, 2017; accepted Jan. 18, 2018.  
Paramvir Kaur Pal (paramvir.kaur@pgr.reading.ac.uk) and Robert Simon Sherratt (corresponding author, r.s.sherratt@reading.ac.uk) are with the Department of Biomedical Engineering, The University of Reading, UK.

This is an Open Access article distributed under the term of Korea Open Government License (KOGIL) Type 4: Source Indication + Commercial Use Prohibition + Change Prohibition (<http://www.kogil.or.kr/info/licenseTypeEn.do>).

Thus, it is possible to improve the received signal power, in a similar manner to beamforming arrays. In MIMO-SPAs, the parasitic elements are able to sample the electromagnetic field in a much wider space compared to the conventional MIMO systems made of active elements only. This technique helps to achieve independent fading by transmitting/receiving different signal paths at each antenna.

The pattern diversity antennas allow a number of uncorrelated patterns per antenna element, to optimally tune the wireless channel for the highest spectral efficiency [6], [7]. By choosing the antennas patterns carefully, it is possible to achieve significantly improved performance by orienting the antennas such that they have diverse radiation patterns with appropriate angles [8]–[10]. Several studies of MIMO systems have shown the benefits of pattern diversity through practical measurements with array designs that employ SPAs [11], [12]. On the other hand, carefully adjusting the radiation patterns of different antennas has the potential to reduce channel correlation and improve multiplexing gain. By properly selecting the array configuration using SPAs, it is possible to choose the channel scenario that allows for the highest throughput in MIMO wireless communication systems [13].

The MIMO channel generally includes the propagation environment, as well as the physical transmit and receive antenna array designs. Changes to any of these subsystems can significantly impact the channel capacity. MIMO systems allow a growth in transmission rate that is linear in terms of the minimum number of antennas at each end of the wireless link [14]. This performance enhancement strongly depends on the quality of the channel state information (CSI) which is available at the transmitter and the receiver links. The best performance can be achieved when such CSI is complete and perfect at both ends of the communication link. However, this is not practically feasible, especially at the transmitter side owing to feedback overhead and bandwidth requirements. However, this can be achieved with the knowledge of the covariance matrix, and can be fed back to the transmitter [15].

The eigenvalue spread (EVS) of the covariance matrix is the most widely used indicator of spatial selectivity to estimate the effective spatial links that are possible within a MIMO system [16]. The two important MIMO channel metrics based on eigenvalues are the rank and condition number (CN), and they reveal important MIMO system characteristics in the spatial domain. The rank of the transmission matrix indicates the number of data streams that can be spatially multiplexed on a MIMO link. However, it does not give any indication about the quality

of the channel matrix, whether it is a well-conditioned or ill-conditioned channel. CN indicates the channel quality [17], [18], and is related to the EVS of the channel matrix. A high EVS indicates that the channel is correlated with a high condition number, and this is referred to as an ill-conditioned channel matrix. Thus, small variations in the channel coefficients will result in drastic variations at the receiver side, making the system unstable. Most of the research work uses the CN as a selection criterion for several purposes. Heath and Paulraj [19] used a CN of the MIMO channel to perform switching between diversity and multiplexing gain purposes. In a similar way, Piazza et al. [20] used a CN to switch between different modes of circular patch reconfigurable antennas. For the adaptive modulation scheme, CN was used by Forenza et al. to obtain the spatial selectivity of the channel [21]. In other studies [22], [23], the regular CN (or its reciprocal) was used to evaluate the quality of the channel matrix as it provides some intuition on channel quality. Thus, the CN can indicate the quality of the MIMO channel to the transmitter using fewer bits, and can overcome the feedback bandwidth requirements.

The feedback mechanism can be more rigorously designed and is more feasible in practice if the dynamic behaviour of the eigenvalues is known statistically. In the absence of the CSI at the transmitter, the best strategy for power allocation is to distribute the power evenly across the antennas. In a high signal-to-noise ratio (SNR) regime, greater capacity can be achieved if the eigenvalues are less spread out. However, in a low-SNR regime, the optimal policy is to inject power into the strongest eigenvalue only, as in the case of beamforming. By using the ‘water-pouring algorithm (WPA),’ the channel capacity can be achieved if the transmission power distributed on the eigenvalues is based on the quality of the channel [24].

The focus of this paper is to propose the use of SPAs in MIMO systems with the knowledge of channel correlation in the form of the covariance matrix. In comparison to conventional MIMO, MIMO-SPAs need a smaller number of RF chains, which reduces cost, space, and hardware complexity. Using parasitic elements, it is possible to perform switching between different radiation patterns by changing the terminated impedance loads separately without affecting the transceiver design. This paper uses the increment antenna selection technique (I-AST) with WPA for proper power allocation in order to achieve the MIMO channel capacity. A CN is also proposed as a selection criterion to select the optimal pattern configuration at the receiver side by using the exhaustive search method. The results show that the channel capacity has been improved by using a covariance matrix for

optimal power allocation compared to the conventional means with equal power allocated across all the transmit antennas.

This paper is organized as follows: Section II describes the overall MIMO system model, Section III presents details of parasitic antenna theory with different pattern configurations, and Section IV shows simulation results of the MIMO channel capacity with the knowledge of different covariance matrices. Finally, Section V concludes the paper.

## II. MIMO System Model

A typical MIMO communication link consists of  $M_T$  transmit and  $N_R$  receive antennas, and the resulting MIMO channel can be described by an  $M_T \times N_R$  channel matrix  $\mathbf{H}$ , whose  $(ij)$ th entry characterizes the path between the  $j$ th transmit and the  $i$ th receive antenna.  $\mathbf{Z}_{T_x}$  and  $\mathbf{Z}_{R_x}$  represent the impedance matrices on the transmitter and receiver sides, respectively [25]. Using Thevenin's theorem, the  $M_T$  sources at the transmitter side can be represented as an ideal voltage in series with lumped impedance  $\mathbf{Z}_S$ . The input current can be found as [7]:

$$\tilde{\mathbf{I}}_S = (\mathbf{Z}_{T_x} + \mathbf{Z}_S)^{-1} \tilde{\mathbf{V}}_S, \quad (1)$$

where  $\tilde{\mathbf{I}}_S = [I_{S1}, I_{S2}, \dots, I_{SM_T}]^T$ ,  $\tilde{\mathbf{V}}_S = [V_{S1}, V_{S2}, \dots, V_{SM_T}]^T$ , and  $\mathbf{Z}_S = \text{diag}(Z_{S1}, Z_{S2}, \dots, Z_{SM_T})$ .

As previously shown [7], assume an operator  $\mathbf{G}$  that relates the gap current vector  $\tilde{\mathbf{I}}_S$  to the vector  $\tilde{\mathbf{V}}_O = [V_{O1}, V_{O2}, \dots, V_{ON_R}]^T$ . Thus, the voltage at the  $N_R$  receiving antennas is:

$$\tilde{\mathbf{V}}_O = \mathbf{G} \tilde{\mathbf{I}}_S. \quad (2)$$

At the receiver side, the open-circuit voltage vector  $\tilde{\mathbf{V}}_O$  is related to the voltages  $\tilde{\mathbf{V}}_R$  with the receiver impedances  $\mathbf{Z}_L$  as follows:

$$\tilde{\mathbf{V}}_R = \mathbf{Z}_{R_x} (\mathbf{Z}_{R_x} + \mathbf{Z}_L)^{-1} \tilde{\mathbf{V}}_O, \quad (3)$$

where  $\tilde{\mathbf{V}}_R = [V_{R1}, V_{R2}, \dots, V_{RN_R}]^T$ ,  $\mathbf{Z}_L = \text{diag}(Z_{L1}, Z_{L2}, \dots, Z_{LN_R})$ , and  $\mathbf{Z}_{R_x}$  is the impedance matrix of the receiving array.

A direct relation between the transmitting and receiving voltages can be obtained as [7]:

$$\tilde{\mathbf{V}}_R = \mathbf{Z}_{R_x} (\mathbf{Z}_{R_x} + \mathbf{Z}_L)^{-1} \mathbf{G} (\mathbf{Z}_{T_x} + \mathbf{Z}_S)^{-1} \tilde{\mathbf{V}}_S = \tilde{\mathbf{H}} \tilde{\mathbf{V}}_S, \quad (4)$$

where  $\mathbf{Z}_S$  and  $\mathbf{Z}_L$  are the controlling load impedances at the transmitter and receiver sides, respectively. Thus, if the number of parasitic elements changes, there will only be a change in the impedance matrices in the design. It is not possible to calculate voltages across parasitic elements directly, and it can thus be calculated as:

$$\mathbf{V}_R = \mathbf{S}_R \tilde{\mathbf{H}} \tilde{\mathbf{V}}_S, \quad (5)$$

where  $\mathbf{S}_R$  is a permutation matrix. Further the values of  $\tilde{\mathbf{H}}$  that are relative to active elements at the receiver side are extracted. If the parasitic elements are connected to the transmitting side, then  $Z_{S_i}$  is the variable impedance that controls the elements, and  $V_{S_i} = 0$ . The voltage at the receiver side can thus be described as:

$$\mathbf{V}_R = \mathbf{S}_R \tilde{\mathbf{H}} \mathbf{S}_T \mathbf{V}_S = \mathbf{H} \mathbf{V}_S, \quad (6)$$

where  $\mathbf{S}_T$  is a permutation matrix, and extract the values of  $\tilde{\mathbf{H}}$  that are relative to active elements at the transmitter side, and  $\mathbf{V}_S$  is the vector of the voltages at the transmitter. In (6),  $\mathbf{H}$  corresponds to the channel matrix of the suggested MIMO system. As the parasitic elements are not connected to any RF source, the output cannot be observed directly on the parasitic elements, but can be collected at the active elements owing to the strong electromagnetic coupling effect. The MIMO system using SPA will provide different channel matrices  $\mathbf{H}$  depending on the number of parasitic elements and the number of states of parasitic loads at the transmitter and receiver sides.

In this paper, parasitic elements are used only at the receiver side for simplicity, thus changing the loads of impedance matrix  $\mathbf{Z}_L$ . It is also possible to change the parasitic controlling impedances at the transmitter side, such as at a base station, but it will significantly impact all of the users at the receiver side.

When communicating over MIMO fading channels,  $\mathbf{H}$  is a random matrix that depends on the specific system architecture and the specific propagation conditions. Hence,  $\mathbf{H}$  is considered to be obtained from a certain probability distribution, which characterizes the system and scenario of interest, and is known as the MIMO channel matrix. In MIMO wireless communications, the large number of scatterers in the channel, which contribute to the signal at the receiver, results in zero-mean Gaussian distributed channel matrix coefficients. The highest channel capacity in the ideal case is possible with a rich scattering environment, where it ensures that all of the channel coefficients of the channel matrix are uncorrelated.

The transmitted symbol vector  $\mathbf{s}$ , which is composed of  $M_T$  independent input symbols  $s_1, s_2, \dots, s_{M_T}$ , is transmitted from  $M_T$  active transmit antennas. Then, the received signal can be written as follows:

$$\mathbf{y} = \sqrt{\frac{E_s}{M_T}} \mathbf{H} \mathbf{s} + \mathbf{n}, \quad (7)$$

where  $\mathbf{n} = (n_1, n_2, \dots, n_{N_R})^T$  is a noise vector, which is assumed to be a zero-mean circular symmetric complex Gaussian. The autocorrelation of the transmitted signal vector is defined as:  $\mathbf{R}_{ss} = E\{ss^H\}$ . The total transmission power for each transmit antenna is assumed to be 1, such as  $\text{Tr}(\mathbf{R}_{ss}) = M_T$ .

When the CSI is available at the transmitter side, singular value decomposition (SVD) can be performed to identify the number of independent equations out of multiple equations of the MIMO system. Accordingly, the transmitted signal can be pre-processed with  $\mathbf{V}$  in the transmitter, and then the received signal can be post-processed with  $\mathbf{U}^H$ . The output of the MIMO system can be described as:

$$\tilde{\mathbf{y}} = \sqrt{\frac{E_s}{M_T}} \mathbf{U}^H \mathbf{H} \mathbf{V} \tilde{\mathbf{s}} + \tilde{\mathbf{n}}. \quad (8)$$

Using the SVD model, the number of MIMO channels is divided into a number of independent SISO channels. The channel matrix  $\mathbf{H} \in \mathbb{C}^{M_T \times N_R}$  with SVD can be represented as:

$$\mathbf{H} = \mathbf{U} \mathbf{\Sigma} \mathbf{V}^H, \quad (9)$$

where  $\mathbf{U} \in \mathbb{C}^{N_R \times N_R}$  and  $\mathbf{V} \in \mathbb{C}^{M_T \times M_T}$  are unitary matrices, and  $\mathbf{\Sigma} \in \mathbb{C}^{M_T \times N_R}$  is a rectangular matrix whose diagonal elements are non-negative real numbers, and whose off-diagonal elements are zero. The diagonal elements of  $\mathbf{\Sigma}$  are the singular values of the matrix  $\mathbf{H}$ , and are denoted by  $\sigma_1, \sigma_2, \dots, \sigma_{\min}$ , where  $N_{\min} \triangleq \min(M_T, N_R)$ . In fact,  $\sigma_1 \geq \sigma_2 \geq \dots \geq \sigma_{\min}$ , that is, the diagonal elements of  $\mathbf{\Sigma}$ , are the ordered singular values of the matrix  $\mathbf{H}$ . The rank of  $\mathbf{H}$  corresponds to the number of non-zero singular values, such that  $\text{rank}(\mathbf{H}) \leq N_{\min}$ .

The MIMO channel capacity is evaluated using Shannon's theory as follows [26]:

$$C = E \left\{ \max_{\text{Tr}(\mathbf{R}_{ss})=M_T} \log_2 \det \left( \mathbf{I}_{N_R} + \frac{E_s}{M_T N_0} \mathbf{H} \mathbf{R}_{ss} \mathbf{H}^H \right) \right\}, \quad (10)$$

where  $E_s$  is the total transmitted power, and  $N_0$  is the variance of the additive white Gaussian noise at the receiver. In a flat-fading MIMO system, channel matrix  $\mathbf{H}$  is a Rayleigh fading model with independent distribution. The covariance matrix  $\mathbf{R}_{ss}$  should be determined in order to satisfy the transmitter power constraints. If the CSI is known at the transmitter, then WPA can be used by employing the increment antenna selection technique (I-AST) to improve the channel capacity.

### III. Parasitic Array Theory

The Yagi-Uda antenna is a linear multi-element array [27], and consists of one active dipole and a

number of parasitic dipoles. The parasitic dipoles are placed close to the active element, so that strong currents are induced in them. The SPA concept originates from the Yagi-Uda dipole array. Electromagnetic mutual coupling has been used as a design tool in order to meet the antenna requirements. The distribution of the currents on the parasitic elements of the array can be carefully designed by adjusting the spacing between the elements and the length of the parasitic dipoles. In the case of the Yagi-Uda antennas, the lengths of all elements are mechanically fixed with different sizes. However, in SPA, the variation of the parasitic elements' electrical equivalent lengths enables the parasitic elements to be switched between the reflector and director state by using the switches [28].

When the RF switch is in the OFF state, the corresponding parasitic element is open-circuited and acts as a director. Therefore, the parasitic element does not have a resonant length, and a minimal amount of current is induced into it. When the switch is in the ON state, the corresponding parasitic element is short-circuited and acts as a reflector. Therefore, the parasitic element acquires a resonant length and strong currents are induced in it. By simply changing the position of the ON/OFF switches, a number of diverse radiation patterns can therefore be created in different angular directions. The most common antenna structure used for this purpose is the circular array [29]. In this case, active elements are placed at the center, and a number of parasitic elements are evenly spaced on the periphery of a circle with radius  $d$ , around the active elements. Parasitic arrays also have symmetrical properties if there is an even number of parasitic elements.

In this paper, the total number of the parasitic elements is assumed to be  $P$ , and the number of possible states of the impedance load on the parasitic elements is denoted by  $L_S$ . The total number of combinations that can be attained by changing the load states of the parasitic elements are [28]:

$$\text{Total combinations} = (L_S)^P. \quad (11)$$

With  $P = 2$  and  $L = 2$ , there are total four combinations, as shown in Fig. 1. These combinations are achieved by changing the impedance loads of parasitic elements between  $Z_{ON}$  and  $Z_{OFF}$ . The ON state is represented by binary "1," and the OFF state is represented by binary "0."

The active elements are driven by voltages  $V_1$  and  $V_2$ .  $I_1$  and  $I_2$  represent the current across the two elements, and are calculated by solving the network equations:

$$\begin{aligned} V_1 &= Z_{11}I_1 + Z_{12}I_2 + \dots + Z_{1N}I_N, \\ V_2 &= Z_{21}I_1 + Z_{22}I_2 + \dots + Z_{2N}I_N, \\ &\vdots \\ V_N &= Z_{N1}I_1 + Z_{N2}I_2 + \dots + Z_{NN}I_N. \end{aligned} \tag{12}$$

$$\begin{bmatrix} V_1 \\ V_2 \\ 0 \\ \vdots \\ V_N \end{bmatrix} = \begin{bmatrix} Z_{11} & Z_{12} & Z_{13} & \dots & Z_{1N} \\ Z_{21} & Z_{22} & Z_{23} & \dots & Z_{2N} \\ Z_{31} & Z_{32} & Z_{33} + Z_{L3} & \dots & Z_{3N} \\ \vdots & \vdots & \vdots & \ddots & \vdots \\ Z_{N1} & Z_{N2} & Z_{N3} & \dots & Z_{NN} + Z_{LN} \end{bmatrix} \begin{bmatrix} I_1 \\ I_2 \\ I_3 \\ \vdots \\ I_N \end{bmatrix} \tag{15}$$

Alternatively, (12) can be written in matrix form, which is normally referred to as the impedance matrix equation:

$$\begin{bmatrix} V_1 \\ V_2 \\ \vdots \\ V_N \end{bmatrix} = \begin{bmatrix} Z_{11} & Z_{12} & \dots & Z_{1N} \\ Z_{21} & Z_{22} & \dots & Z_{2N} \\ \vdots & \vdots & \ddots & \vdots \\ Z_{N1} & Z_{N2} & \dots & Z_{NN} \end{bmatrix} \begin{bmatrix} I_1 \\ I_2 \\ \vdots \\ I_N \end{bmatrix}, \tag{13}$$

or can be written as [28]:

$$\mathbf{V} = [\mathbf{Z} + \mathbf{Z}_L]\mathbf{I}, \tag{16}$$

where  $\mathbf{Z}_L$  is the diagonal matrix consisting of the impedance loads across the terminal of each passive element:

$$\mathbf{Z}_L = \begin{bmatrix} 0 & 0 & 0 & \dots & 0 \\ 0 & 0 & 0 & \dots & 0 \\ 0 & 0 & Z_{L3} & \dots & 0 \\ \vdots & \vdots & \vdots & \ddots & \vdots \\ 0 & 0 & 0 & \dots & Z_{Lp} \end{bmatrix}, \tag{17}$$

which can also be represented as:

$$\mathbf{V} = \mathbf{Z}\mathbf{I}, \tag{14}$$

where  $\mathbf{V}$  is the column vector of the excitation voltages  $V_i$ , for  $i = 1, 2, \dots, N$ .  $\mathbf{Z}$  is the square impedance matrix, which is formed by the self and mutual impedances of the elements of the array.  $\mathbf{I}$  is the column vector of the complex currents along the array elements. In this paper, there are two active elements present at the receiver side. The active elements are typically terminated with 50-Ω loads, and parasitic elements are terminated with the impedance loads:

where  $Z_{Lp}$  is the impedance load connected to the  $p$ th parasitic element in the array. In the load matrix  $\mathbf{Z}_L$ , all the diagonal entries except the first two are non-zero. The first two entries are zero because the active elements are not connected to any controllable impedance loads. This load matrix can be computed separately from the impedance matrix. This feature is beneficial because the impedance loads of the individual parasitic elements can be changed separately. The new impedance matrix is computed using the induced electromagnetic force (EMF) method [27] by adding the initial impedance matrix and the load matrix. Once the impedance matrix is computed, the individual element's current excitations can be calculated easily.

The dipole antennas are used as antenna array elements to generate different radiation patterns using the EMF method [27], as shown in Fig. 1. The structural parameters were calculated based on the array theory [28]. Here, the variable impedances have only two different levels ( $Z_{ON}, Z_{OFF}$ ), which give  $(L_S)^P$  different pattern configurations. Thereafter, all of the antenna attributes, including radiation patterns, can be calculated.

#### IV. Results

In this work, MIMO systems have two transmitting and two receiving antennas with the channel matrix  $\mathbf{H}$  ( $2 \times 2$ ), but using switched parasitic elements ( $P = 2$ ) at the receiver side only.

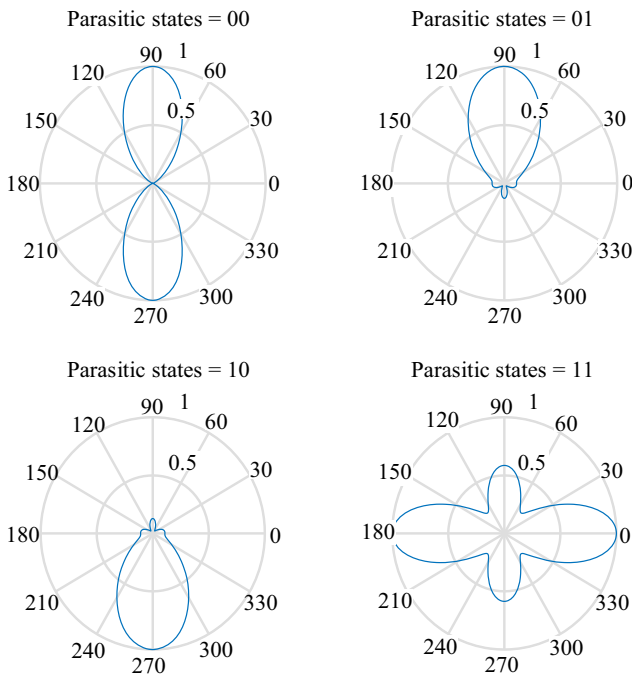


Fig. 1. Typical radiation patterns for load configurations.

The simulation scenario for a MIMO system ( $2 \times 2$ ) using two parasitic elements at the receiver side only is given as follows:

- Number of active elements on the transmitter side  $M_{ta} = 2$
- Number of active elements on the receiver side  $N_{ra} = 2$
- Number of parasitic elements on the transmitter side  $M_{tp} = 0$
- Number of parasitic elements on the receiver side  $N_{rp} = 2$
- Total number of elements on the transmitter side  $M_T = M_{ta} + M_{tp} = 2$
- Total number of elements on the receiver side  $N_R = N_{ra} + N_{rp} = 4$

Two parasitic antennas with ON/OFF states give four different pattern configurations on the receiver side. In MIMO-SPAs, there are four different channel matrices ( $\mathbf{CH}_{00}, \mathbf{CH}_{01}, \mathbf{CH}_{10}, \mathbf{CH}_{11}$ ), according to the state of the switches (ON/OFF). The channel matrix ( $\mathbf{CH}_{00}$ ), when both of the parasitic elements switches are in the OFF state, is similar to the conventional MIMO (without using any parasitic elements).

With the knowledge of these matrices, it is possible to evaluate the Shannon’s channel capacity as follows [24]:

$$C = \log_2 \left( I_{N_r} + \frac{E_s}{M_T N_0} \mathbf{H} \mathbf{R}_{ss} \mathbf{H}^H \right). \quad (18)$$

The covariance matrix  $\mathbf{R}_{ss}$  should be determined to satisfy the transmitter power constraints. With four different channel matrices, the MIMO channel capacity will be different across each pattern configuration. The more the channel is correlated, the lower will be the channel capacity.

### 1. Influence of Covariance Matrix

It is well known that the covariance matrix can change the channel capacity mainly according to the power allocation at the transmitter side by using SVD [24].

To determine the effect of the covariance matrix on the MIMO channel capacity, two different propagation medium cases can be analyzed:

- i. Uncorrelated
- ii. Correlated.

In the uncorrelated case, the covariance matrix is an identity matrix. The diagonal elements of the matrix  $\mathbf{R}_{ss}$  are 1’s and all other elements are zeros. This means that all of the channel coefficients are uncorrelated. Thus, equal power is allocated to all of the transmit antennas. Figure 2 shows that the ergodic channel capacity increases with respect to SNR in the uncorrelated case.

In the correlated case, all the elements of the covariance matrix are set to 1. This means that all of the channel coefficients are correlated. The channel capacity decreases with respect to SNR owing to the correlation effect, as shown in Fig. 3. The high correlation provided by the matrix  $\mathbf{R}_{ss}$ , represents a negative influence on the channel capacity.

If the channel conditions are known to the transmitter, then the incremental/decremental antenna-selection techniques can be applied with the WPA for proper power

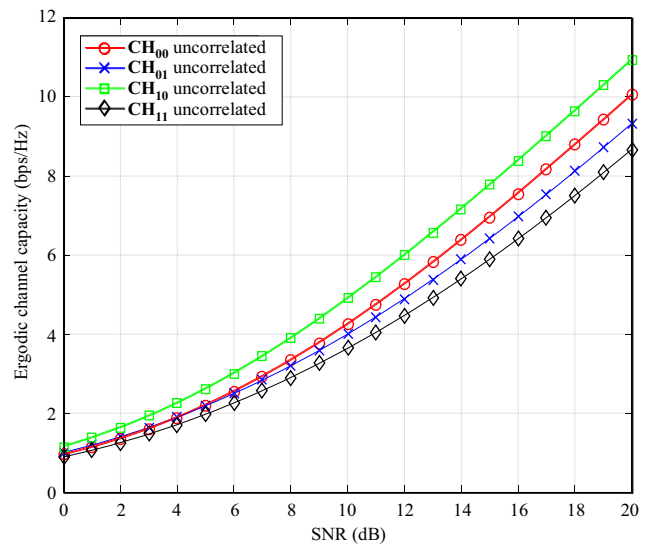


Fig. 2. Channel capacity using identity matrix as covariance matrix.

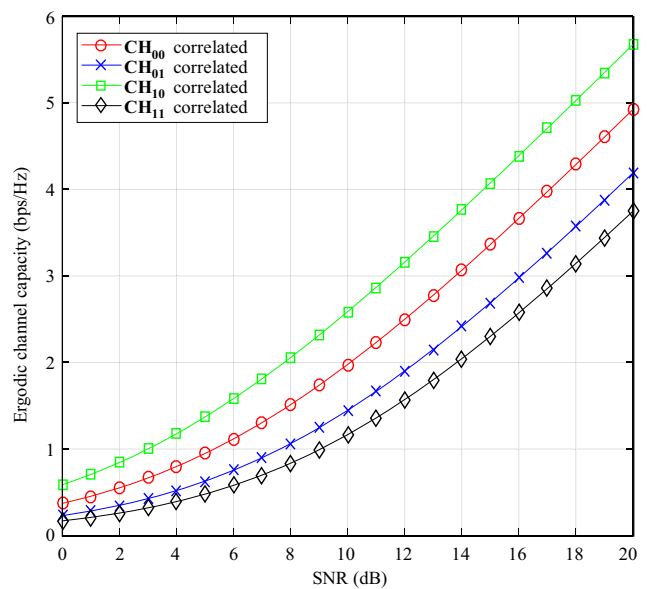


Fig. 3. Channel capacity using matrix of all ones as covariance matrix.



allocation at the transmitter side. The knowledge of the channel conditions can be fed back to the transmitter in the form of a covariance matrix. The covariance matrix

represents the correlation present in the channel, and with WPA, more power can be distributed to the best channel, and less power to channels that contribute less to the channel capacity.

A comparison of four different configurations for the uncorrelated case with and without WPA is shown in Fig. 4. For all of the parasitic configurations, the MIMO channel capacity is improved with the power allocation using WPA as compared to the equal power distribution across all the eigenvalues.

### 2. Comparison of Different Covariance Matrices

In this section, the I-AST is used to select the best set of antennas, and then allocates power by carrying out WPA.

The comparison between covariance matrices across all the pattern configurations is shown in Fig. 5. The comparison is discussed with three different covariance matrices as follows:

- I-AST with correlated covariance matrix-  $[\mathbf{R}_{ss}]_{\text{corr}}$
- I-AST with uncorrelated covariance matrix-  $[\mathbf{R}_{ss}]_{\text{uncorr}}$
- I-AST with improved covariance matrix WPA-  $[\mathbf{R}_{ss}]_{\text{WPA}}$

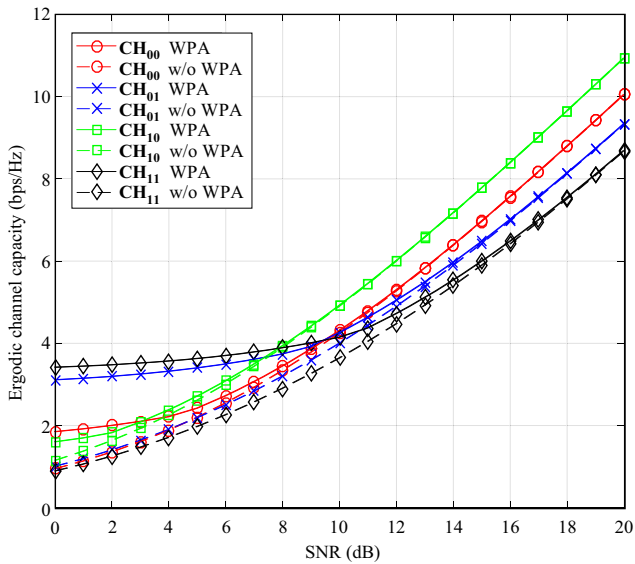


Fig. 4. Comparison of all pattern configuration matrices with and without WPA.

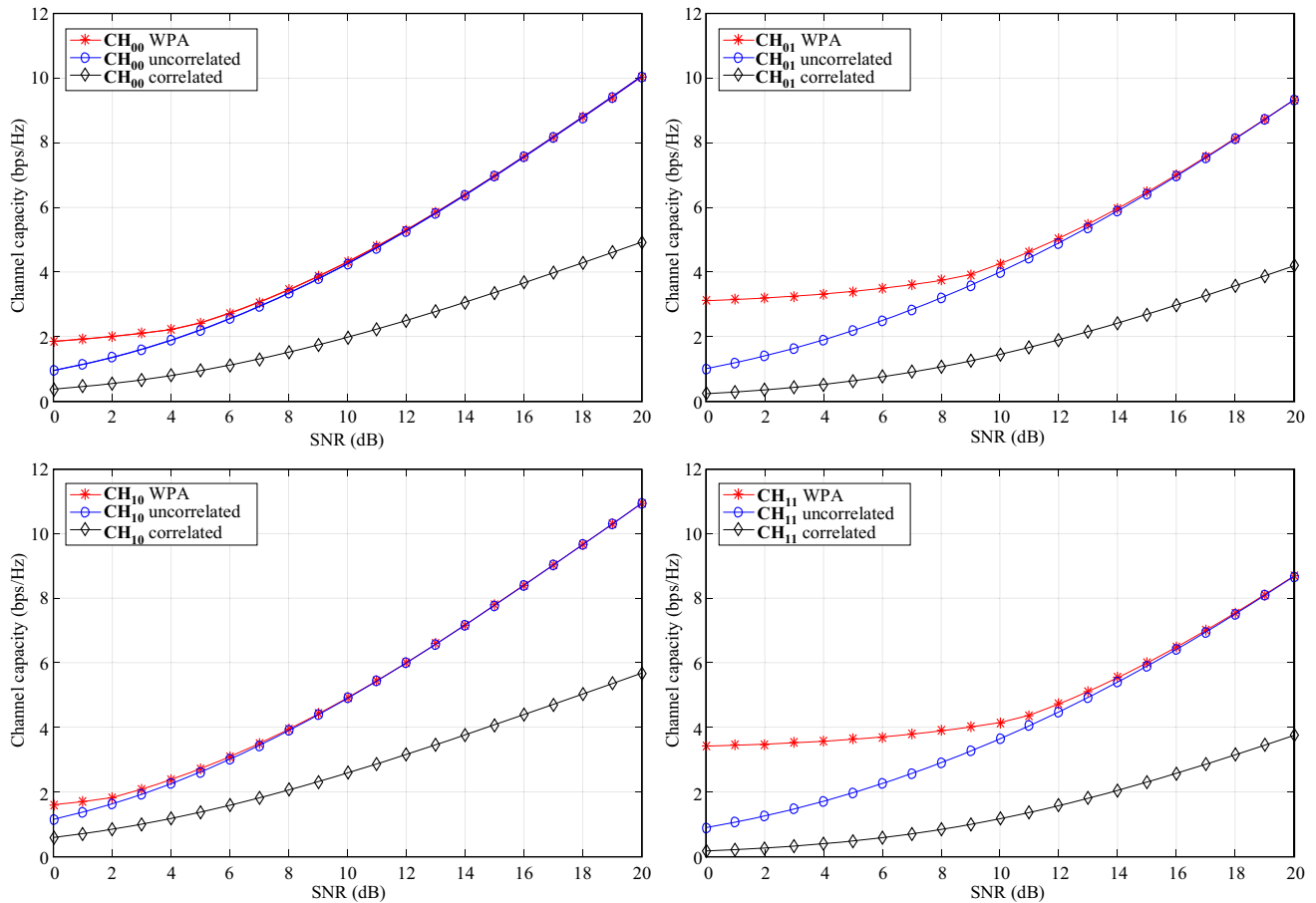


Fig. 5. Comparison of channel capacity with three different forms of covariance matrices across all pattern configurations.

In this comparison, when the channel matrix is correlated, it gives the lower bounds for the MIMO channel capacity for all of the pattern configurations. When the channel matrix is uncorrelated with I-AST, the channel capacity is improved compared to the correlated case. Figure 5 shows that when the covariance matrix is improved with WPA, in all different configuration matrices, the channel capacity provides the upper bounds. These are the bounds according to the influence of the covariance matrix in three different cases.

### 3. Pattern Configuration Selection

CN is known as the channel quality indicator and used to obtain the best pattern configuration. It represents the EVS of the channel as [15]:

$$CN = \frac{\lambda_{\max}}{\lambda_{\min}}, \quad (19)$$

where  $\lambda_{\max}$  and  $\lambda_{\min}$  are the maximum and minimum eigenvalues of the covariance matrix, respectively.

If eigenvalues of the covariance matrix are less spread out, it provides a small CN value. In MIMO-SPAs, there are four different pattern configurations. All four pattern configurations represent the four different channel matrices ( $\mathbf{CH}_{00}$ ,  $\mathbf{CH}_{01}$ ,  $\mathbf{CH}_{10}$ ,  $\mathbf{CH}_{11}$ ), and have different CNs. By performing the exhaustive search, the channel matrix or pattern that has a low CN is selected. For the selection purpose in the uncorrelated case, as shown in Fig. 5, the pattern configuration  $\mathbf{CH}_{10}$  matrix with the lowest CN is selected. This is the optimal pattern configuration with the best channel quality, and provides

the greatest channel capacity compared with other configurations.

### 4. Pattern Configuration for Different SNR Values

The MIMO channel capacity also depends on the SNR values. The behavior of four pattern configurations at different SNRs levels are shown in Fig. 6. It can be seen that at 5 dB–15 dB, the second pattern configuration  $\mathbf{CH}_{01}$  provides the highest channel capacity. At 20 dB and 25 dB, the third configuration  $\mathbf{CH}_{10}$  can be selected as it provides the highest channel capacity.

## V. Conclusion

SPAs offer a significant advantage in terms of the use of handheld devices, where space, cost, and hardware complexity are the primary constraints. The main advantages of SPAs are their ability to change their radiation pattern and to operate within a specific changing environment, while maintaining good electromagnetic characteristics. For simplicity, and to provide a limited level of pattern diversity, only two switch positions (ON/OFF) were used in this study.

Based on the knowledge of the channel statistics, a decomposition model decouples the transmit signal into orthogonal eigenbeams. The power distribution assigned to these eigenvalues is according to the WPA, which means that there is a greater power in directions where the channel is strong, but reduced or no power in directions with weak channels. Using the I-AST technique with WPA, the MIMO-SPAs channel capacity is significantly improved for all the pattern configurations. A comparison of three covariance matrices showed that the improved power allocation of the covariance matrix with WPA has a higher channel capacity than others.

The novel contribution of this paper is the use of the CN as a selection criterion to determine the optimal pattern configuration for the receiver antenna array. The behavior of the CN of the covariance matrix represents the EVS of the channel. Using a good-quality channel, a high multiplexing gain can be achieved with proper transmission. Thus, the CN is an excellent indicator of channel quality, and is a very useful metric in link adaptation schemes.

In the future, this work will be extended for application to multicarrier systems such as orthogonal frequency-division multiplexing (OFDM), where it is possible to select the pattern selection using the CN across a number of subcarriers. It also has the advantage of feedback and bandwidth reduction in future wireless communication systems.

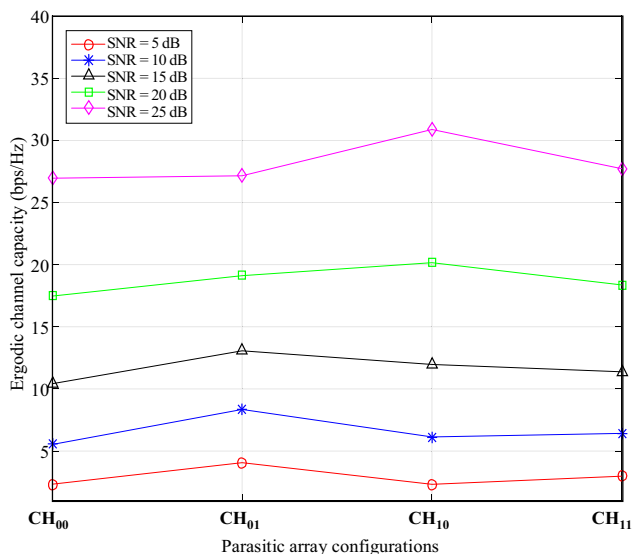


Fig. 6. Pattern configuration selection at different SNR values.



## References

- [1] E. Telatar, "Capacity of Multi-antenna Gaussian Channel," *Trans. Emerg. Telecommun. Technol.*, vol. 10, no. 6, Nov. 1999, pp. 585–595.
- [2] G.J. Foschini and M.J. Gans, "On Limits of Wireless Communications in a Fading Environment When Using Multiple Antennas," *Wireless Personal Commun.*, vol. 6, no. 3, Mar. 1998, pp. 311–335.
- [3] R. Vaughan, "Switched Parasitic Elements for Antenna Diversity," *IEEE Trans. Antennas Propag.*, vol. 47, no. 2, Feb. 1999, pp. 399–405.
- [4] M. Wennstrom and T. Svantesson, "An Antenna Solution for MIMO Channels: The Switched Parasitic Antenna," *IEEE Int. Symp. Personal, Indoor Mobile Radio Commun.*, San Diego, CA, USA, Sept. 2001, pp. 159–163.
- [5] A. Kalis, A.G. Kanatas, and C.B. Papadias, "A Novel Approach to MIMO Transmission Using a Single RF Front End," *IEEE J. Sel. Areas Commun.*, vol. 26, no. 6, Aug. 2008, pp. 972–980.
- [6] A. Kalis, A.G. Kanatas, and C.B. Papadias, *Parasitic Antenna Arrays for Wireless MIMO Systems*, New York, USA: Springer, 2014.
- [7] M.D. Migliore, D. Pinchera, and F. Schettino, "Improving Channel Capacity Using Adaptive MIMO Antennas," *IEEE Trans. Antennas Propag.*, vol. 54, no. 11, Nov. 2006, pp. 3481–3489.
- [8] O.N. Alrabadi, C. Divarathne, P. Tragas, A. Kalis, N. Marchetti, C.B. Papadias, and R. Prasad, "Spatial Multiplexing with a Single Radio: Proof-of-Concept Experiments in an Indoor Environment with a 2.6 GHz Prototype," *IEEE Commun. Lett.*, vol. 15, no. 2, Feb. 2011, pp. 178–180.
- [9] O.N. Alrabadi, J. Perruisseau-Carrier, and A. Kalis, "MIMO Transmission Using a Single RF Source: Theory and Antenna Design," *IEEE Trans. Antennas Propag.*, vol. 60, no. 2, Feb. 2012, pp. 654–664.
- [10] D. Gwak, I. Sohn, and S.H. Lee, "Analysis of Single-RF MIMO Receiver with Beam-Switching Antenna," *ETRI J.*, vol. 37, no. 4, Aug. 2015, pp. 647–656.
- [11] R. Bains and R. Muller, "Using Parasitic Elements for Implementing the Rotating Antenna for MIMO Receivers," *IEEE Trans. Wirel. Commun.*, vol. 7, no. 11, Nov. 2008, pp. 4522–4533.
- [12] M. DiZazzo, M.D. Migliore, F. Schettino, V. Patriarca, and D. Pinchera, "A Novel Parasitic-MIMO Antenna," *IEEE Antennas Propag. Soc. Inter. Symp.*, Albuquerque, NM, USA, July 2006, pp. 4447–4450.
- [13] M. Yoshida, K. Sakaguchi, and K. Araki, "Single Front-End MIMO Architecture with Parasitic Antenna Elements," *IEICE Trans. Commun.*, vol. E95-B, no. 3, Mar. 2012, pp. 882–888.
- [14] M. Vu and A. Paulraj, "MIMO Wireless Linear Precoding," *IEEE Signal Process. Mag.*, vol. 24, no. 5, Sept. 2007, pp. 86–105.
- [15] D. Sacristán-Murga and A. Pascual-Iserte, "Differential Feedback of MIMO Channel Gram Matrices Based on Geodesic Curves," *IEEE Trans. Wirel. Commun.*, vol. 9, no. 12, Dec. 2010, pp. 3714–3727.
- [16] D. Tse and P. Viswanath, *Fundamentals of Wireless Communication*, Cambridge, UK: Cambridge University Press, 2005.
- [17] J. Zik, *Maximizing LTE Performance through MIMO Optimization*, Germantown, PA, USA: PCTEL Inc., Apr. 2011.
- [18] M. Zia, T. Kiani, H. Mahmood, T. Shah, and N.A. Saqib, "Bandwidth-Efficient Selective Retransmission for MIMO-OFDM Systems," *ETRI J.*, vol. 37, no. 1, Feb. 2015, pp. 66–76.
- [19] R.W. Heath and A.J. Paulraj, "Switching Between Diversity and Multiplexing in MIMO Systems," *IEEE Trans. Commun.*, vol. 53, no. 6, 2005, pp. 962–968.
- [20] D. Piazza, J. Kountouriotis, M. D'Amico, and K.R. Dandekar, "A Technique for Antenna Configuration Selection for Reconfigurable Circular Patch Arrays," *IEEE Trans. Antennas Propag.*, vol. 8, no. 3, Mar. 2009, pp. 1456–1467.
- [21] A. Forenza, A. Pandharipande, H. Kim, and R.W. Heath, "Adaptive MIMO Transmission Scheme: Exploiting the Spatial Selectivity of Wireless Channels," *IEEE Veh. Technol. Conf.*, Stockholm, Sweden, May 30–June 1, 2005, pp. 3188–3192.
- [22] D. Pinchera and M.D. Migliore, "Effectively Exploiting Parasitic Arrays for Secret Key Sharing," *IEEE Trans. Veh. Tech.*, vol. 65, no. 1, Jan. 2016, pp. 123–131.
- [23] R.W. Heath and D.J. Love, "Multimode Antenna Selection for Spatial Multiplexing Systems with Linear Receivers," *IEEE Trans. Signal Process.*, vol. 53, no. 8, Aug. 2005, pp. 3042–3056.
- [24] J.V. Cuan-Cortes, C. Vargas-Rosales, and D. Munoz-Rodriguez, "MIMO Channel Capacity Using Antenna Selection and Water Pouring," *EURASIP J. Wirel. Commun. Netw.*, vol. 2014, Dec. 2014, pp. 1–10.
- [25] C.A. Balanis, *Antenna Theory*, New York, USA: Wiley, 2005.
- [26] C.E. Shannon, "A Mathematical Theory of Communication," *Bell Syst. Tech. J.*, vol. 27, no. 3, 1948, pp. 379–423.
- [27] S.J. Orfanidis, "Electromagnetic Waves and Antennas," Rutgers University, 2002, pp. 702–733, Accessed 2017. <http://www.ece.rutgers.edu/~orfanidi/ewa/>

- [28] M.R.O. Mofolo, A.A. Lysko, T.O. Olwal, and W.A. Clarke, "Beam Steering for Circular Switched Parasitic Arrays Using a Combinational Approach," *IEEE AFRICON*, Livingstone, Zambia, Sept. 13–15, 2011, pp. 1–6.
- [29] K. Gyoda and T. Ohira, "Design of Electronically Steerable Passive Array Radiator (ESPAR) Antennas," *IEEE Antennas Propag. Soc. Int. Symp.*, Salt Lake City, UT, USA, July 16–21, 2000, pp. 922–925.



**Paramvir Kaur Pal** received her BEng degree in electronics engineering from Nagpur University, India, in 2001, and her MEng degree in electronics from Punjab Engineering College, Chandigarh, India in 2004. From 2004 to 2006, she worked as a lecturer at the Shaheed Udham Singh College of Engineering and Technology, Mohali, India. She is currently pursuing her PhD degree at the University of Reading, UK. Her research interests are in the area of MIMO wireless communication for closely spaced antennas and spatial multiplexing.



**Robert Simon Sherratt** received his BEng degree in electronic systems and control engineering from Sheffield City Polytechnic, UK, in 1992, and his MSc and PhD degrees in electronic engineering from the University of Salford, UK, in 1994 and 1996, respectively. From 1996, he has been with the University of Reading, UK, where he is now a full professor. His research areas are signal processing and personal communications in consumer devices, focusing on wearable devices for healthcare applications.